Talanta 81 (2010) 901–907

Contents lists available at ScienceDirect

Talanta

journal homepage: www.elsevier.com/locate/talanta

Ultrasensitive fluorometric determination of hydrogen peroxide and glucose by using multiferroic $BiFeO_3$ nanoparticles as a catalyst

Wei Luo[a], Yu-Sang Li[b,*], Jing Yuan[a,c], Lihua Zhu[a,**], Zhengdan Liu[a], Heqing Tang[a], Shusheng Liu[c]

[a] College of Chemistry and Chemical Engineering, Huazhong University of Science and Technology, Wuhan 430074, PR China
[b] College of Pharmacy, South-Central University for Nationalities, Wuhan 430074, PR China
[c] Key Laboratory of Yangtze River Water Environment, Ministry of Education, College of Environmental Science and Engineering, Tongji University, Shanghai 200092, PR China

ARTICLE INFO

Article history:
Received 4 November 2009
Received in revised form 15 January 2010
Accepted 17 January 2010
Available online 25 January 2010

Keywords:
Hydrogen peroxide
Glucose
Catalysis
$BiFeO_3$
Fluorometric
Benzoic acid

ABSTRACT

$BiFeO_3$ magnetic nanoparticles (BFO MNPs) are used as a catalyst to develop an ultrasensitive method for the determination of H_2O_2. It is found that BFO MNPs can catalyze the decomposition of H_2O_2 to produce •OH radicals, which in turn oxidize the weakly fluorescent benzoic acid to a strongly fluorescent hydroxylated product with a maximum emission at 405 nm. This makes it possible to sensitively quantify traces of H_2O_2. Under optimized conditions, the fluorescence intensity is observed to be well linearly correlated with H_2O_2 concentration from 2.0×10^{-8} to 2.0×10^{-5} mol L^{-1} with a detection limit of 4.5×10^{-9} mol L^{-1} (S/N = 3). In addition, a selective method for glucose determination is developed by using both glucose oxidase and BFO MNPs, which has a linear range for glucose concentration from 1.0×10^{-6} to 1.0×10^{-4} mol L^{-1} with a detection limit of 5.0×10^{-7} mol L^{-1}. These new methods have been successfully applied for the determination of H_2O_2 in rainwater and glucose in human serum samples.

1. Introduction

Glucose is one of the most important carbohydrates and functions as a source of energy in living bodies. The amount of glucose in the human blood stays within narrow limits throughout a day (4.0–8.0 mmol L^{-1}) [1]. In recent years, the determination of glucose has gained tremendous importance in biomedical analysis for effective treatment of prediabetes and diabetes [2]. In biochemical analysis, glucose is mainly measured by monitoring H_2O_2 being stoichiometrically produced during its oxidation by dissolved oxygen in the presence of glucose oxidase (GOx) [3–6]. Hence, H_2O_2 is an important yardstick for glucose determination. Therefore, it is of interesting to develop a reliable and sensitive analytical method for the precise monitoring of H_2O_2.

H_2O_2 performs an important role in atmospheric and biochemical processes [7]. It was proved to be the most efficient oxidant for the conversion of dissolved sulfur dioxide (SO_2) to sulfuric acid (H_2SO_4). The formed H_2SO_4 is the main contributor to the acid rainwater, causing a serious environmental problem over the world [8–10]. Thus, the concentration of H_2O_2 in rainwater is an important indicator providing information of the environment. H_2O_2 is also a by-product in the oxidation metabolic process, which is harmful to the organism and causes damage to the body when its concentration reaches 0.5 mmol L^{-1} [11]. Several methods have been investigated to detect H_2O_2, including titrimetry [12], fluorometry [11,13–15], spectrophotometry [16,17], chemiluminescence [18,19], and electrochemistry [20–22]. Among these techniques, the horseradish peroxidase (HRP)-catalyzed reaction is one of the most widely used enzymatic reactions. Based on HRP, various sensitive fluorometric methods have been developed for the H_2O_2 determination [23,24]. Although HRP is of high specificity and sensitivity, its instability and high cost restrict its application [25].

Recently, functional nanomaterials have received considerable attention in catalysis due to their large surface-to-volume ratio [26,27]. Yan and co-workers found that Fe_3O_4 MNPs exhibit catalytic ability for the activation of H_2O_2 [28]. Wang and co-worker used Fe_3O_4 MNPs as a catalyst to detect H_2O_2 with a linear range from 5.0×10^{-6} to 1.0×10^{-4} mol L^{-1} [29]. We used Fe_3O_4 MNPs as a catalyst and developed a sensitive spectrophotometric method for the detection of H_2O_2 in a linear range from 5.0×10^{-7} to 1.5×10^{-4} mol L^{-1} with a detection limit of 2.5×10^{-7} mol L^{-1} [17]. As an extension to our recent work [17], we are trying to find more efficient H_2O_2-activation catalysts and develop an ultrasensitive fluorometric method for the determination of H_2O_2.

* Corresponding author. Tel.: +86 27 67842332; fax: +86 27 67842332.
** Corresponding author at: College of Chemistry and Chemical Engineering, Huazhong University of Science and Technology, 1037 Luo-Yu Road, Hongshan Qu, Wuhan 430074, China. Tel.: +86 27 87543432; fax: +86 27 87543632.
E-mail addresses: liys2006@yahoo.cn (Y.-S. Li), lhzhu63@yahoo.com.cn (L. Zhu).

0039-9140/$ – see front matter © 2010 Elsevier B.V. All rights reserved.
doi:10.1016/j.talanta.2010.01.035

Multiferroic magnetic nanoparticles, such as BFO MNPs, have attracted significant attention for various applications including data storage, spin valves, and sensor [30–34]. In the present work, we explored the catalytic effect of BFO MNPs and made use of the BFO MNPs as a nonenzymatic catalyst for the detection of H_2O_2. The BFO MNPs were prepared by a modified sol–gel method and were used to catalyze the conversion of weakly fluorescent benzoic acid (BA) to strong fluorescent hydroxylated benzoic acid (OHBA) in the presence of H_2O_2. The fluorescence intensity of the product OHBA (Ex 295 nm, Em 405 nm) was found to be proportional to the concentration of H_2O_2. Therefore, an ultrasensitive fluorometric method for the determination of H_2O_2 was developed on the basis of the BFO MNPs (Eq. (1)):

$$H_2O_2 + BA \xrightarrow{\text{BFO MNPs}} OHBA \quad (1)$$

$$O_2 + \text{glucose} \xrightarrow{\text{GOx}} H_2O_2 + \text{gluconic acid} \quad (2)$$

By coupling the oxidation of glucose catalyzed by GOx (Eq. (2)) with the BA oxidation catalyzed by BFO MNPs (Eq. (1)), a fluorometric method was further developed for quantitative analysis of glucose, which was observed to have a linear range from 1.0×10^{-6} to 1.0×10^{-4} mol L^{-1} and a detection limit of 5.0×10^{-7} mol L^{-1} glucose.

2. Experimental

2.1. Reagents and solutions

Iron nitrate ($Fe(NO_3)_3 \cdot 9H_2O$), bismuth nitrate ($Bi(NO_3)_3 \cdot 5H_2O$), glucose and benzoic acid were obtained from Tianjin Chemical (Tianjin, China). Ethylene glycol, 2-methoxyethanol, trichloroacetic acid, methylene blue (MB) and 30% (w/w) H_2O_2 were provided by Sinopharm Chemical Reagent Co., Ltd. (Shanghai, China). Potassium permanganate ($KMnO_4$), Na_2HPO_4, NaH_2PO_4 and citric acid were bought from Shanghai Chemical (Shanghai, China). HRP (specific activity of 300 units mg^{-1}, RZ ≥ 3) and GOx were purchased from Tianyuan Biologic Engineering Corp (China). *N*,*N*-Diethyl-*p*-phenylenediamine sulfate (DPD) and 5,5-dimethyl-1-pyrroline *N*-oxide (DMPO) were purchased from Aldrich. All reagents were of analytical grade and used as received. Double distilled water was used in the present work. H_2O_2 stock standard solution (0.01 mol L^{-1}) was prepared from 30% H_2O_2 solution and standardized by titration with $KMnO_4$ (0.021 mol L^{-1}). 2.20 g Na_2HPO_4 and 0.40 g NaH_2PO_4 prepared in 100 mL distilled water were mixed in order to yield a PBS buffer solution (pH 7.0). The freshly prepared H_2O_2 stock standard solution was stored in an amber-glass bottle at 4 °C prior to experiment. Diluted solutions of H_2SO_4 and NaOH (1.0 mol L^{-1}) were used to adjust solution pH.

2.2. Apparatus and measurement procedures

Morphology of $BiFeO_3$ sample was observed on a Hitachi S-4300 SEM instrument at an acceleration voltage of 15 KV. ESR spectra were obtained on a Bruker ESR 300E with microwave bridge (receiver gain, 1×10^5; modulation amplitude, 2 Gauss; microwave power, 10 mW; modulation frequency, 100 kHz).

The MB degradation experiments were carried out in a cylindrical vessel (75 mL). BFO MNPs were dispersed into 50 mL of dye MB aqueous solution to form suspension which was sonicated for 1 min and magnetically stirred in dark for 30 min to attain the adsorption/desorption equilibrium. After this period, the degradation reaction was initiated by adding 0.5 mL of 1.0 mol L^{-1} H_2O_2 and carried out under stirring condition. Solution samples were taken at a given time intervals during the reaction, and immediately centrifuged at 14,000 rpm for 3 min using an EBA-21 centrifugal (Hettich, Germany) to remove BFO MNPs. The supernatant was further filtered with a 0.22 μm filter, and the MB concentration in the filtrate was determined by using a UV–visible spectrophotometer (Varian Cary 50, USA).

Unless specified elsewhere, the basic reaction conditions for determination of H_2O_2 were set as follows: initial $BiFeO_3$ concentration 0.5 g L^{-1}, initial BA concentration 1.0 mmol L^{-1}, reaction time 20 min, and initial solution pH 3.0. After the reaction was ended, the resultant OHBA solution was adjusted to pH 10.0 by adding 1 mol L^{-1} NaOH, and then the fluorescence intensity (Ex 295 nm, Em 405 nm) was determined on a FP-6200 fluorescence spectrophotometer (Jasco, Japan). Based on these measurements, a linear correlation between the fluorescence intensity and H_2O_2 concentration was established. Rainwater samples were collected in three different glass beakers (0.5 L) and were filtered through a 0.22 μm filter before the analysis of H_2O_2 concentration. Human serum samples were provided by Wuhan Centers for Disease Prevention and Control. In order to eliminate the possible interference of proteins in human serum, the fresh serum samples were pretreated with 0.5 mol L^{-1} trichloroacetic acid to precipitate the proteins, and then centrifuged at 14,000 rpm for 20 min and the supernatant was collected.

For glucose analysis, standard glucose solution (or diluted serum sample, 1.00 mL), GOx solution (5 U mL^{-1}, 0.20 mL), PBS buffer solution (pH 7.0, 0.50 mL) and H_2O (0.80 mL) were mixed and incubated at 30 °C for 30 min. After that, BFO MNPs (2.50 g L^{-1}, 1.00 mL) and BA (3.30 mmol L^{-1}, 1.50 mL) solutions were added. The mixed solution was further adjusted to pH 3.0 by adding 1.0 mol L^{-1} H_2SO_4 and allowed to react for 20 min, and then centrifuged at 14,000 rpm for 3 min to remove BFO MNPs. Finally, the supernatant was adjusted pH to 10.0 by adding 1.0 mol L^{-1} NaOH and used to analyze the fluorescence intensity at 405 nm. All the prepared samples were stored in an amber-glass bottle at 4 °C for prior to the analysis. Each experiment was repeated three times to ensure the reproducibility, and the experimental data were averaged.

2.3. Preparation of $BiFeO_3$ nanoparticles

In a typical preparation, iron(III) nitrate (3.232 g, 0.008 mol) and bismuth nitrate (3.880 g, 0.008 mol) were dissolved in 20 mL 2-methoxyethanol, followed by adding 20 μL of 0.1 mol L^{-1} HNO_3. Then, citric acid (1.680 g, 0.008 mol) was added to the solution as a complexant, and ethylene glycol (10 mL) was introduced as a dispersant to the above mixture [33]. The solution was stirred until the dissolution was completely achieved. Next, the mixture was stirred for one hour at 60 °C to form a sol, which was then kept at 100 °C for 10 h to obtain a dark viscous resin. The resin was heated for 5 min on an electric furnace to obtained gel powders, and then calcined at 500 °C for 2 h in a muffle furnace.

3. Result and discussion

3.1. Characterization of BFO MNPs by SEM

It is known that the catalytic activity of a heterogeneous catalyst strongly dependent on the shape, size and size distribution of the particles. Fig. 1 shows the SEM image of the BFO MNPs. It is clearly seen that the powders are composed of aggregated extremely fine particles with a narrow nano-size distribution (grain sizes of 100–150 nm), being favorable to a highly efficient catalytic effect of BFO MNPs as a heterogeneous catalyst.

3.2. Activation of H_2O_2 in the presence of BFO MNPs catalyst

The reduction of H_2O_2 is thermodynamically favored, but it is a slow process in conventional solutions in the absence of any cata-

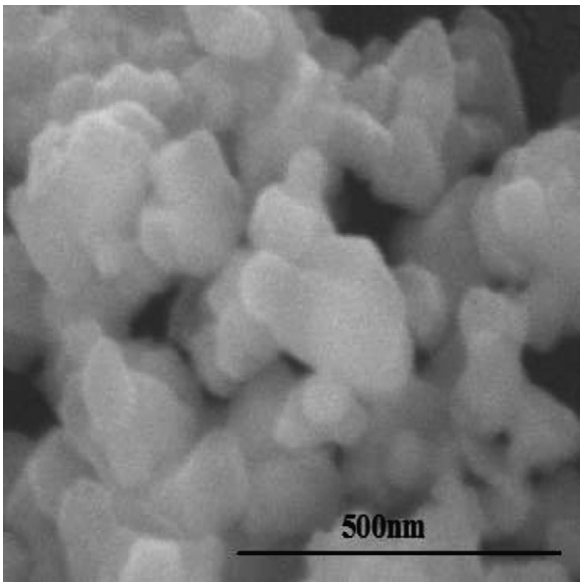

Fig. 1. SEM image of $BiFeO_3$ nanoparticles.

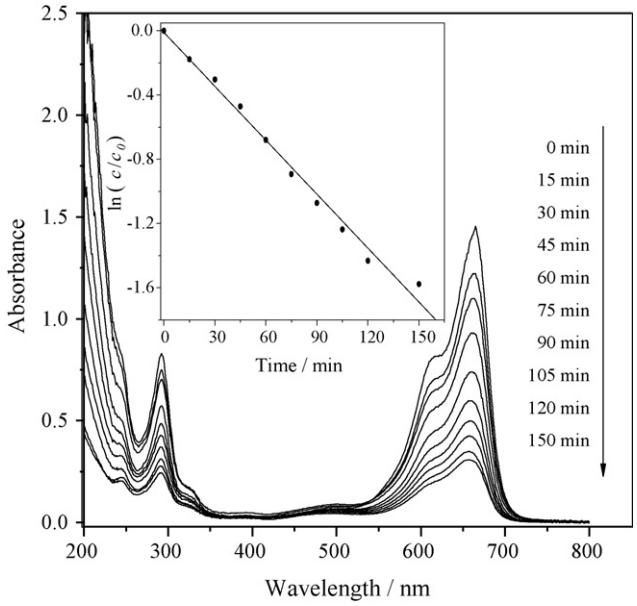

Fig. 2. UV–vis absorption spectra of MB (20 μmol L^{-1}) solution during the oxidation in the presence of H_2O_2 (10.0 mmol L^{-1}) and BFO MNPs (0.5 g L^{-1}) at pH 7.2. The inset gives the kinetic data for the degradation of MB.

lysts. Transition-metal ions and their complexes may catalyze the H_2O_2 activation. As a natural enzyme, HRP with the heme iron acts as the activity center is the most commonly used enzyme in H_2O_2 activation and detection [35]. To mimic the activity center of natural peroxidases, a number of synthesized complexes containing iron(III) or iron(II) at their reaction centers have been recently developed and showed effective capability for H_2O_2 activation [36–38]. However, most of these complexes are difficult to be massively synthesized due to the difficulty in the preparation of the organic ligands, and the organic complex catalyst itself may be decomposed due to the slow degradation of the organic ligands during the activation of H_2O_2. Therefore, it is very interesting to develop all-inorganic, efficient and reusable catalysts for H_2O_2 activation because these catalysts will have the merits of easy preparation and improved stability. BFO MNPs are one of such candidates.

In order to evaluate the efficiency of BFO MNPs in the activation of H_2O_2, the dye MB was used as the model of organic compounds, and the MB degradation was carried out in a cylindrical vessel, being monitored by UV–vis absorption measurement. As shown in Fig. 2, the absorption peak at 292 nm is assigned to the aromatic rings and the peak at 662 nm is assigned to the conjugated structure formed by the azo bond. The decrease in the absorbance at 662 nm is due to the degradation of MB. Although MB was not degraded in the presence of either BFO MNPs or H_2O_2 alone (data not shown), the simultaneous presence of BFO MNPs and H_2O_2 has removed 79.5% of MB within 150 min (Fig. 2). The MB degradation obeys a pseudo-first-order reaction in kinetics as shown in the inset of Fig. 2, which gives the rate constant as 0.0113 min^{-1}. This strongly confirms that BFO MNPs possess catalytic activity for activation of H_2O_2.

The mechanism of H_2O_2 activation by BFO MNPs may involves the initial formation of a complex between ≡Fe(III) and H_2O_2, which is assigned as ≡Fe(III)H_2O_2, here ≡Fe(III) stands for the iron(III) ions in the surface of BFO MNPs catalyst. The initially generated ≡Fe(III)H_2O_2 species are converted to ≡Fe(II) species and $^{\bullet}HO_2$, and the generated $^{\bullet}HO_2$ reacted with ≡Fe(III) to produce ≡Fe(II) species. All the formed ≡Fe(II) species further reacted with H_2O_2 to generate $^{\bullet}$OH radicals. This mechanism is in accordance with the observations of Kwan and Voelker [39] and Molina and co-workers [40], who reported that iron oxide catalyzed the production of $^{\bullet}$OH radicals from H_2O_2. We used the DMPO spin-trapping ESR technique to detect whether the BFO MNPs–H_2O_2 system could produce any $^{\bullet}$OH radicals or not during the catalysis. The ESR spectra (curve a in Fig. 3) displayed a 4-fold characteristic peak of the typical DMPO–$^{\bullet}$OH adduct with an intensity ratio of 1:2:2:1, while no such signal was found in the absence of BFO MNPs (curve b in Fig. 3), providing that the $^{\bullet}$OH radicals were the main active species in this system.

The generation of $^{\bullet}$OH radicals is very important for the analysis of H_2O_2. Because the generated $^{\bullet}$OH radicals can react with weakly fluorescent BA to produce fluorescent adduct OHBA, which shows strong fluorescence at 405 nm when excited at 295 nm (Fig. 4). The fluoresence intensity of OHBA is found to be proportional to the concentration of H_2O_2, which lead to develop a sentive, stable and selective fluorometric method for the H_2O_2 determination.

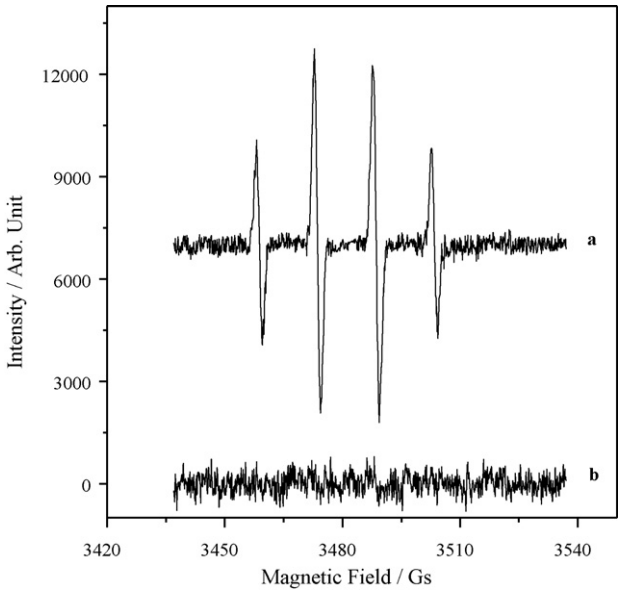

Fig. 3. ESR spectra of hydroxyl radicals in the systems of (a) 0.5 g L^{-1} BFO MNPs, 10.0 mmol L^{-1} H_2O_2 and 1.0 mmol L^{-1} BA, (b) 10.0 mmol L^{-1} H_2O_2 and 1.0 mmol L^{-1} BA.

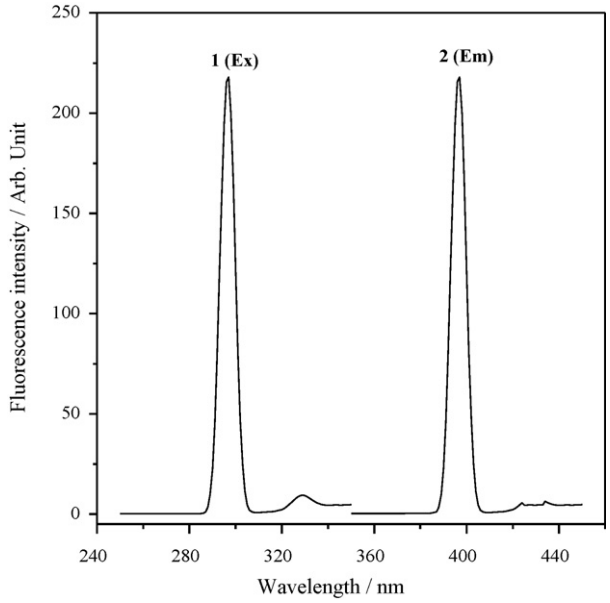

Fig. 4. Excitation (1) and emission (2) spectra of the BA–H_2O_2–BFO MNPs system. Reaction conditions: 0.5 g L^{-1} BFO MNPs, 2.0×10^{-5} mol L^{-1} H_2O_2, 1.0 mmol L^{-1} BA, pH 3.0, and reaction time 20 min. Measurement conditions: excitation at 295 nm, and emission at 405 nm.

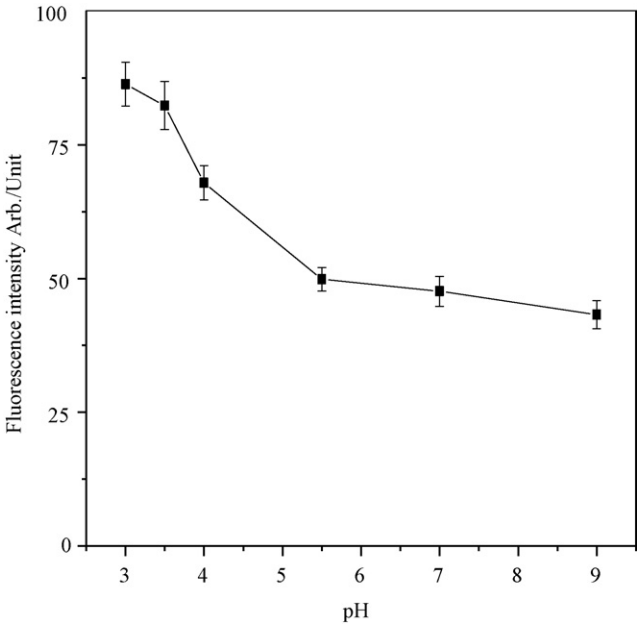

Fig. 6. Effect of pH on the fluorescence intensity. Reaction conditions: 0.5 g L^{-1} BFO MNPs, 5.0×10^{-6} mol L^{-1} H_2O_2, 1.0 mmol L^{-1} BA, and reaction time 20 min. Measurement conditions: excitation at 295 nm, and emission at 405 nm.

3.3. *Effects of operation parameters on the determination of H_2O_2*

In order to optimize the possible analytical method for the H_2O_2 determination, the effects of experimental conditions including reaction time, solution pH, initial BA concentration, and initial BFO MNPs concentration were investigated.

3.3.1. *Effect of reaction time*

The effect of reaction time was investigated at given conditions (pH 3.0, 0.5 g L^{-1} BFO MNPs, 1.0 mmol L^{-1} BA, 5.0×10^{-6} mol L^{-1} H_2O_2). As shown in Fig. 5, the fluorescence intensity of the generated OHBA is rapidly increased with the reaction time initially, and then tends to saturate beyond 15 min. The "saturation" of the fluorescence intensity beyond 15 min indicates that the added H_2O_2 is completely consumed by the oxidation of the substrate BA. Hence, a reaction time is optimized as 20 min to reduce the total operation time in the present work.

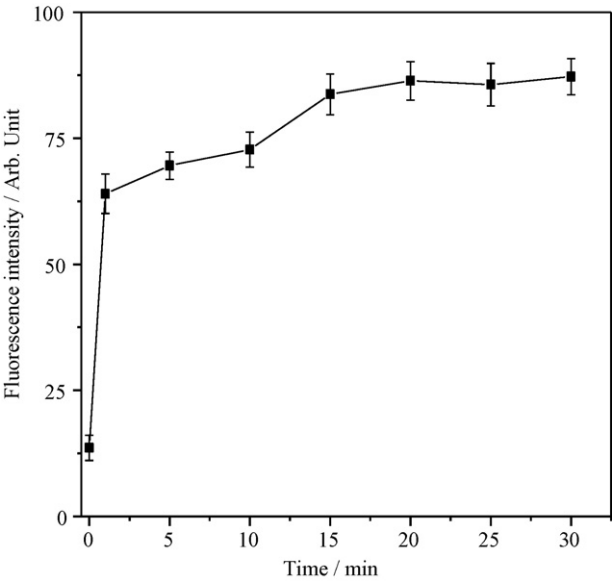

Fig. 5. Effect of reaction time on the fluorescence intensity. Reaction conditions: 0.5 g L^{-1} BFO MNPs, 5.0×10^{-6} mol L^{-1} H_2O_2, 1.0 mmol L^{-1} BA, pH 3.0. Measurement conditions: excitation at 295 nm, and emission at 405 nm.

3.3.2. *Effect of pH of reaction solution*

The solution pH is an important factor that affects the catalytic activity of BFO MNPs. It is clear from Fig. 6 that the catalytic oxidation of BA by H_2O_2 with BFO MNPs as the catalyst is much faster in acidic solutions than in neutral and basic solutions. It seems that the reaction solution pH should be as low as possible for the determination of H_2O_2. However, the BFO MNPs are not so stable in strongly acidic conditions due to the acidic leaching of iron components in the BFO MNPs. Therefore, the solution pH was selected at pH 3.0 for further experiments.

3.3.3. *Effect of initial BA concentration*

The reactant BA is a weakly fluorescent, but the product OHBA is highly fluorescent. Thus, the excess of BA will not influence the measurement of the fluorescence intensity of the reaction solution. Fig. 7 illustrates the influence of BA concentration on the fluorescence intensity of the reaction solution. For a given concentration of H_2O_2 (5.0×10^{-6} mol L^{-1}), the fluorescence intensity is enhanced with increasing of BA concentration up to 0.75 mmol L^{-1}, and then keeps almost constant beyond 0.75 mmol L^{-1} of BA. The apparent saturation of the fluorescence intensity is attributed to a complete reduction of H_2O_2 in the reaction system. In order to expand the linear range for the determination of H_2O_2, we selected a moderately higher concentration of BA (1.0 mmol L^{-1}) for the further experiments.

3.3.4. *Effect of the load of BFO MNPs*

The effect of the BFO MNPs load is studied as shown in Fig. 8. For a given H_2O_2 concentration of 5.0×10^{-6} mol L^{-1} at pH 3.0, the generation of OHBA is significantly promoted initially with increasing of BFO MNPs load, and then kept almost constant beyond 0.5 g L^{-1} of BFO MNPs. Thus, the load of BFO MNPs is selected at 0.5 g L^{-1} for the determination of H_2O_2.

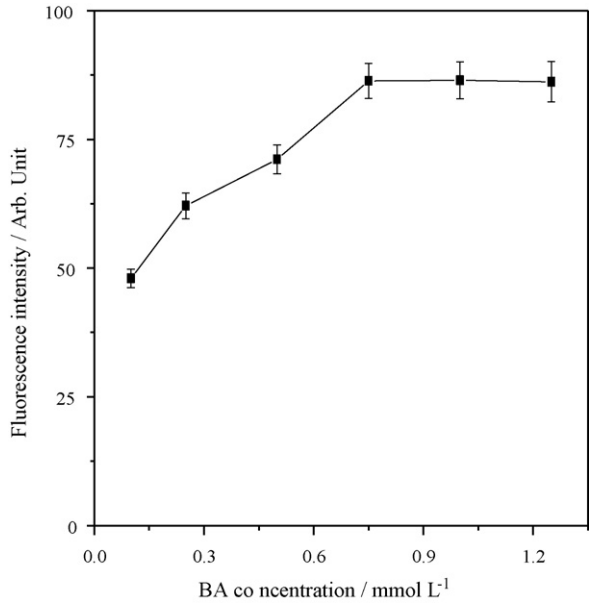

Fig. 7. Effect of BA concentration on the fluorescence intensity. Reaction conditions: 0.5 g L^{-1} BFO MNPs, 5.0×10^{-6} mol L^{-1} H_2O_2, pH 3.0, and reaction time 20 min. Measurement conditions: excitation at 295 nm, and emission at 405 nm.

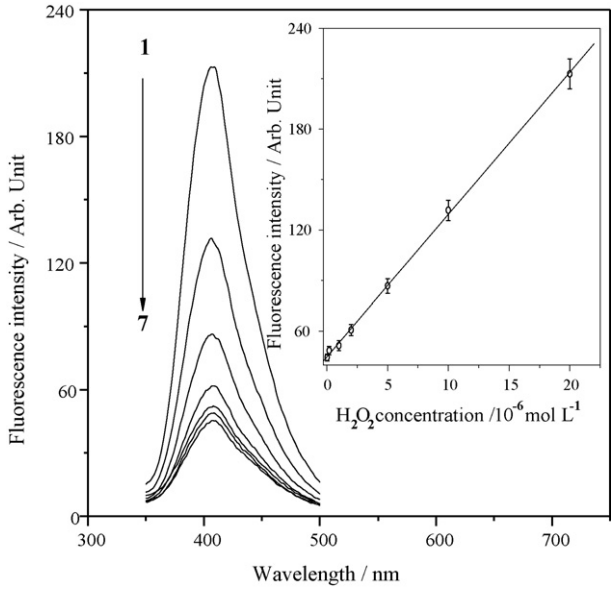

Fig. 9. Emission spectra of the BA–BFO MNPs system containing various concentrations of H_2O_2 (20, 10, 5, 2, 1, 0.2, and 0.02 μmol L^{-1} for the spectra from the top to the bottom). The inset gives the linear correlation between the fluorescence intensity and H_2O_2 concentration. Reaction conditions: 0.5 g L^{-1} BFO MNPs, 1.0 μmol L^{-1} BA, pH 3.0, and reaction time 20 min. Measurement conditions: excitation at 295 nm, and emission at 405 nm.

3.4. Calibration curve for H_2O_2 and glucose detection

Under the optimized reaction conditions (c_{BA} 1.0 mmol L^{-1}, c_{BFO} 0.5 g L^{-1}, pH 3.0 and reaction time 20 min), the calibration curve for the H_2O_2 determination was obtained by establishing a linear correlation between fluorescence intensity (I) at 405 nm and the H_2O_2 concentration (c, mol L^{-1}). Fig. 9 clearly indicates that the correlation is linear in the range of 2.0×10^{-8}–2.0×10^{-5} mol L^{-1} of H_2O_2 with the regression equation of $I = 44.23 + 8.41 \times 10^{-6}\, c$ ($n = 5$) and a correlation coefficient of 0.998. The detection limit was calculated as 4.5×10^{-9} mol L^{-1} (S/N = 3). The relative standard deviation was 3.8% for the determination of 5.0×10^{-6} mol L^{-1} H_2O_2 ($n = 5$).

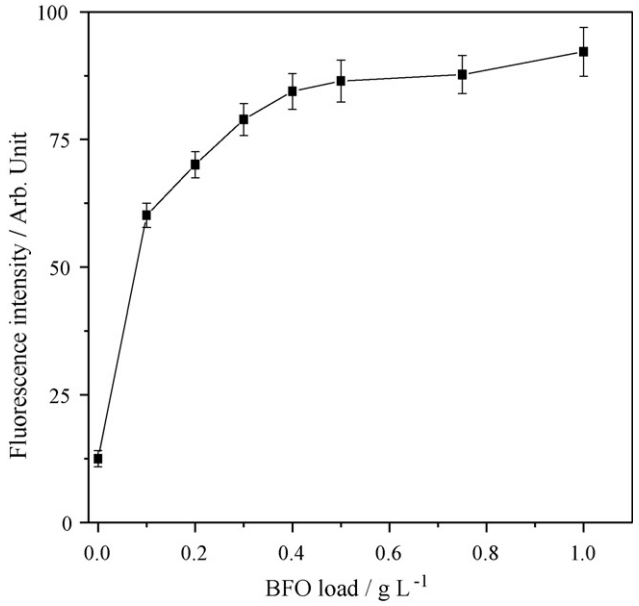

Fig. 8. Effect of BFO MNPs load on the fluorescence intensity. Reaction conditions: 5.0×10^{-6} mol L^{-1} H_2O_2, 1.0 mmol L^{-1} BA, pH 3.0, and reaction time 20 min. Measurement conditions: excitation at 295 nm, and emission at 405 nm.

As mentioned above, when the catalytic reaction (Eq. (1)) is coupled with the catalytic oxidation of glucose by GOx (Eq. (2)), a fluorometric method for the determination of glucose is readily established. Because GOx may be denatured at pH 3.0, the glucose determination was performed in two separated steps as mentioned in the experimental section. In the first step, the catalytic oxidation of glucose in the presence of GOx (Eq. (2)) was carried out in a PBS buffer solution. In the second step, the amount of H_2O_2 produced in the first step was further determined by using BFO MNPs as the catalyst and BA as the organic substrate (Eq. (1)). In this way, a fluorometric method for the determination of glucose has been developed in the present work. Fig. 10 clearly shows that this method has a well linear range from 1.0×10^{-6}

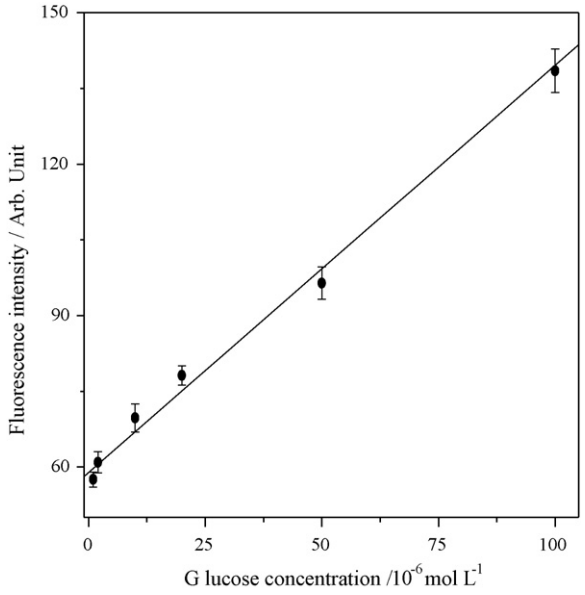

Fig. 10. Calibration plot for glucose determination.

Table 1
Comparison of different methods for the determination of H_2O_2 and glucose.

Methods	Major reagents	Linear range (mol L^{-1})	Detection limit (mol L^{-1})	Reference
Electrochemistry	MWCNTs/MG/HRP[a]	H_2O_2: 5.0×10^{-7}–2×10^{-5}	–	[20]
Electrochemistry	Calyx[4]arene	H_2O_2: 5.5×10^{-4}–6.3×10^{-2} Glucose: 2.5×10^{-4}–1.6×10^{-3}	4.0×10^{-5} 2.0×10^{-5}	[21]
Electrochemistry	Hemoglobin/TiO_2	H_2O_2: 3.0×10^{-6}–1.5×10^{-3}	1.0×10^{-6}	[22]
Spectrophotometry	Fe_3O_4, DPD	H_2O_2: 5.0×10^{-7}–1.5×10^{-4}	2.5×10^{-7}	[17]
Spectrophotometry	Fe_3O_4, ABTS[b]	H_2O_2: 5.0×10^{-6}–1.0×10^{-4} Glucose:5.0×10^{-5}–1.0×10^{-3}	3.0×10^{-6} 3.0×10^{-5}	[29]
Spectrophotometry	Methyl orange, $FeSO_4$	H_2O_2: 5.0×10^{-7}–1.0×10^{-4}	2.0×10^{-7}	[16]
Fluorometry	HRP, Cy.7.Cl[c]	H_2O_2: 1.8×10^{-7}–7.2×10^{-6}	5.6×10^{-8}	[11]
Fluorometry	DI[d]	H_2O_2: 5.0×10^{-7}–9.0×10^{-4}	–	[15]
Fluorometry	Hemoglobin	H_2O_2: 1.0×10^{-7}–8×10^{-5}	2.6×10^{-8}	[14]
Fluorometry	BA, BFO MNPs	H_2O_2: 2.0×10^{-8}–2.0×10^{-5} Glucose:1.0×10^{-6}–1.0×10^{-4}	4.5×10^{-9} 5.0×10^{-7}	This work

[a] MWCNTs: multiwalled carbon nanotubes; MG: methylene green.
[b] ABTS: 2,2-azino-bis(3-ethylbenzo-thiazoline-6-sulfonic acid) diammonium salt.
[c] Cy.7.Cl: tricarbochlorocyanine dye.
[d] DI: 3,3-diethylo-xadicarbocy-anine iodide.

Table 2
Interferences studies for the determination of H_2O_2 (5.0×10^{-6} mol L^{-1}) and glucose (2.0×10^{-5} mol L^{-1}).

Interferents	Molar ratio	$\Delta F\%$	Interferents	Molar ratio	$\Delta F\%$
NaCl	1000	1.21	$MnSO_4$	100	4.57
$NaNO_3$	1000	3.52	Benzene	100	−3.10
$MgSO_4$	1000	2.45	KI	50	−4.92
$(NH_4)_2SO_4$	500	1.76	Vitamin C	5	−2.60
$CaCl_2$	500	2.80	Fructose[a]	75	−5.00
$ZnSO_4$	200	3.95	Maltose[a]	90	4.95
$Na_2C_2O_4$	200	−4.53	L-Phenylalanine[a]	70	−4.97
$Al_2(SO_4)_3$	200	4.22	Arginine[a]	60	−4.98
$CuSO_4$	100	4.86	Glycine[a]	110	4.95
$AgNO_3$	100	3.69			

[a] These compounds were tested as interferents for the determination of glucose.

to 1.0×10^{-4} mol L^{-1} of glucose with a detection limit as low as 5.0×10^{-7} mol L^{-1} (S/N = 3).

Table 1 has summarized the analytical performances of the new methods and previously reported methods for the determination of H_2O_2 and glucose. In comparison with the methods reported in the literature [11,14–17,20–22,29], the method proposed in the present work has the widest linear range and lowest detection limit. Moreover, the reagents used in this method are simple, and the operation procedures for the analysis are very easy.

3.5. Possible interference

The effect of interferents on the determination of hydrogen peroxide (5.0×10^{-6} mol L^{-1}) is shown in Table 2. A relative error of ±5.0% in the change of relative fluorescence intensity ($\Delta F\%$) was considered to be tolerable. As shown in Table 2, various common salts such as NaCl, $NaNO_3$, $MgSO_4$, $(NH_4)_2SO_4$, $CaCl_2$, $ZnSO_4$, $Na_2C_2O_4$, and $Al_2(SO_4)_3$ are allowed to be present at high tolerable molar ratios (>200). However, the tolerable molar ratios are lower for easily oxidized compounds and the salts of some transition-metal ions. The tolerance to reducing agents KI and vitamin C are poorer due to their oxidation by H_2O_2 or •OH radicals. Poorer tolerance to the transition-metal ions (such as Ag(I), Mn(II) and Cu(II)) are possibly attributed to that these ions can catalyze the breakdown of H_2O_2 to generate •OH radicals.

Possible interference of fructose, maltose, L-phenylalanine, arginine and glycine to the determination of glucose (2.0×10^{-5} mol L^{-1}) was also studied as shown in Table 2. It was found that the tolerable molar ratios for these possible interferents are higher than 60. Thus, the new fluorometric method displays high selectivity for the determination of glucose.

3.6. Practical application

This newly developed method was used to determine H_2O_2 in three practical rainwater samples. We also compared our proposed method with a classical DPD method established by Bader et al. [35], in which the H_2O_2-oxidized HRP reacts with DPD to produce a stable purple colored product DPD^+, showing a maximum absorption at 552 nm. For the analysis of the practical rainwater samples, 2.7 mL of the sample was mixed with 0.3 mL PBS buffer solution (pH 7.0), followed by rapid addition of 50 μL DPD (10 g L^{-1}) and 50 μL HRP (0.5 g L^{-1}). The absorption was measured after a reaction time of 1 min. Each sample was analyzed at the same time with both methods in order to avoid any possible differences caused by the degradation of the analyte in the sample. As seen from Table 3, the H_2O_2 concentration was determined as 1.83, 2.15 and 2.38 μmol L^{-1} for the three rainwater samples, respectively. When 1.50 μmol L^{-1} H_2O_2 was added into the rainwater samples, the recoveries of H_2O_2 were found to be ranged from 96.4% to 105.8%. Moreover, there is an excellent agreement between the proposed

Table 3
Determination of H_2O_2 in rainwater samples (n = 5).

Samples	H_2O_2 concentration (μmol L^{-1})		Relative error (%)	F values in F-test[a]	H_2O_2 added (μmol L^{-1})[b]	Recovery[b]
	BA method	DPD method				
1	1.83 ± 0.09	1.90 ± 0.07	3.83	4.85	1.50	96.4
2	2.15 ± 0.13	2.10 ± 0.12	2.33	3.52	1.50	105.8
3	2.38 ± 0.11	2.25 ± 0.09	4.47	4.45	1.50	98.5

[a] For comparison, $F_{(4,4)}$ = 6.39.
[b] By using BA method.

Table 4
Determination of glucose in healthy human serum samples ($n = 3$).

Sample	Add (mmol L^{-1})	Found (mmol L^{-1})[a]	RSD (%)	Recovery (%)
1	0	5.40 (5.25)	3.25	0
	5.00	10.95	4.58	105.3
2	0	4.68 (4.75)	2.36	0
	5.00	9.12	3.57	94.2
3	0	7.43 (7.25)	3.85	0
	5.00	13.02	4.20	104.7

[a] The data in the parentheses were provided by the Hospital of Huazhong University of Science and Technology.

BA method and the classical DPD method (showing an error of less than 4.47% between the two methods). We have also carried out the *F*-test with 95% confidence level to compare the results obtained by the BA method and DPD method in Table 3. The results of the randomization *F*-test shows that, in comparison with the tabulated critical value ($F_{(4,4)} = 6.39$) at the 95% confidence level, all samples are not significant since their *F*-values (4.85, 3.52 and 4.45) are lower than 6.39, which indicate that there are no significant differences between the two methods.

The glucose concentration in three human serum samples was determined with the proposed method after the samples were diluted 40 times. As shown in Table 4, it was found that there were 5.40, 4.68 and 7.43 mmol L^{-1} of glucose in the three serum samples, which are in good agreement with the data provided by the Hospital of Huazhong University of Science and Technology (Wuhan). By adding 5.00 mmol L^{-1} of glucose into the serum samples, the recoveries were observed to be ranged from 94.2% to 105.3%. The results demonstrate that the proposed method can be satisfactorily applied to analyze practical samples.

4. Conclusions

In summary, we developed a simple and novel fluorometric method for the determination of H_2O_2 and glucose on the basis of catalytic activation of H_2O_2 with BFO MNPs as the catalyst at room temperature. The ESR results proved that the catalytic activation of H_2O_2 produced reactive •OH radicals, which oxidized a weakly fluorescent organic substrate BA to strongly fluorescent OHBA, and the fluorescence intensity of OHBA at 405 nm responded linearly well with the concentration of H_2O_2. Under the optimized conditions, a linear correlation was established between the fluorescence intensity and the concentration of H_2O_2 in a range of 2.0×10^{-8}–2.0×10^{-5} mol L^{-1}, with a detection limit of 4.5×10^{-9} mol L^{-1}. This method was easily converted to a new way for the determination of glucose by simultaneously using BFO MNPs and GOx. The new method for the determination of glucose yielded linear responses to glucose concentrations ranging from 1.0×10^{-6} to 1.0×10^{-4} mol L^{-1} with a detection limit of 5.0×10^{-7} mol L^{-1}. The two above-mentioned methods were successfully applied for the determination of H_2O_2 in rainwater and glucose in human serum samples. The present work confirmed that the BFO MNPs possess catalytic ability for the activation of H_2O_2, which have great potential applications in biomaterials, biosensors and environmental sciences.

Acknowledgements

The National Natural Science Foundation of China (Grant Nos. 20877031 and 20677019), and the State Key Laboratory of Pollution Control and Resource Reuse Foundation (No. PCRRF08007) are greatly appreciated for the financial support of this work.

References

[1] P. Nagaraja, A. Shivakumar, A.K. Shrestha, Anal. Biochem. 395 (2009) 231.
[2] P.F. Pang, Y.L. Zhang, S.T. Ge, Q.Y. Cai, S.Z. Yao, C.A. Grimes, Sens. Actuators B 136 (2009) 310.
[3] G.G. Guilbault, P.J. Brignac, M. Zimmer, Anal. Chem. 40 (1968) 190.
[4] D. Lan, B.X. Li, Z.J. Zhang, Biosens. Bioelectron. 24 (2008) 934.
[5] Q. Chang, L. Zhu, G.D. Jiang, H. Tang, Anal. Bioanal. Chem. 395 (2009) 2377.
[6] D. Fink, I. Klinkovich, O. Bukelman, R.S. Marks, A. Kiv, D. Fuks, W.R. Fahrner, L. Alfonta, Biosens. Bioelectron. 24 (2009) 2702.
[7] C.L. Wang, A. Mulchandani, Anal. Chem. 67 (1995) 1109.
[8] Y.G. Zuo, J. Hoigne, Science 260 (1993) 71.
[9] H. Sakugawa, I.R. Kaplan, W. Tsai, Y. Cohan, Environ. Sci. Technol. 24 (1990) 1452.
[10] R.C. Matos, J.J. Pedrotti, L. Angnes, Anal. Chim. Acta 441 (2001) 73.
[11] B. Tang, L. Zhang, K.H. Xu, Talanta 68 (2006) 876.
[12] N.V. Klassen, D. Marchington, H.C.E. Mcgovan, Anal. Chem. 66 (1994) 2921.
[13] J.Z. Li, P.K. Dasgupta, G.A. Tarver, Anal. Chem. 75 (2003) 1203.
[14] C.L. Xu, Z.J. Zhang, Anal. Sci. 17 (2001) 1449.
[15] H.Q. Chen, H.P. Yu, Y.Y. Zhou, L. Wang, Spectrochim. Acta A 67 (2007) 683.
[16] W. Luo, M.E. Abbas, L. Zhu, K. Deng, H. Tang, Anal. Chim. Acta 629 (2008) 1.
[17] Q. Chang, K.J. Deng, L. Zhu, G.D. Jiang, C. Yu, H. Tang, Microchim. Acta 165 (2009) 299.
[18] Y.F. Hu, Z.J. Zhang, C.Y. Yang, Anal. Chim. Acta 601 (2007) 95.
[19] A. Tahirovic, A. Copra, E.O. Miklicanin, K. Kalcher, Talanta 72 (2007) 1378.
[20] A.K. Upadhyay, T.W. Ting, S.M. Chen, Talanta 79 (2009) 38.
[21] G.D. Jin, S. Du, X.Y. Hu, Talanta 80 (2009) 858.
[22] G.D. Jiang, H. Tang, L. Zhu, J.D. Zhang, B. Lu, Sens. Actuators B 138 (2009) 607.
[23] Y.Z. Li, A. Townshend, Anal. Chim. Acta 359 (1998) 149.
[24] J.P.N. Ribeiro, M.A. Segundo, S. Reis, J.L.F.C. Lima, Talanta 79 (2009) 1169.
[25] X. Chen, D. Li, H. Yang, Q. Zhu, H. Zheng, J. Xu, Anal. Chim. Acta 434 (2001) 51.
[26] C. Burda, X.B. Chen, R. Narayanan, M.A. El-Sayed, Chem. Rev. 105 (2005) 1025.
[27] A. Roucoux, J. Schulz, H. Patin, Chem. Rev. 102 (2002) 3757.
[28] L.Z. Gao, J. Zhuang, L. Nie, J.B. Zhang, Y. Zhang, N. Gu, T.H. Wang, J. Feng, D.L. Yang, S. Perrett, X.Y. Yan, Nat. Nanotechnol. 2 (2007) 577.
[29] H. Wei, E.K. Wang, Anal. Chem. 80 (2008) 2250.
[30] J. Wang, J.B. Neaton, H. Zheng, V. Nagarajan, S.B. Ogale, B. Liu, D. Viehland, V. Vaithyanathan, D.G. Schlom, U.V. Waghmare, N.A. Spaldin, K.M. Rabe, M. Wuttig, R. Ramesh, Science 299 (2003) 1719.
[31] T. Zhao, A. Scholl, F. Zavaliche, K. Lee, M. Barry, A. Doran, M.P. Cruz, Y.H. Chu, C. Ederer, N.A. Spaldin, R.R. Das, D.M. Kim, S.H. Baek, C.B. Eom, R. Ramesh, Nat. Mater. 5 (2006) 823.
[32] Y.H. Chu, L.W. Martin, M.B. Holcomb, M. Gajek, S.J. Han, Q. He, N. Balke, C.H. Yang, D. Lee, W. Hu, Q. Zhan, P.L. Yang, A. Fraile-Rodriguez, A. Scholl, S.X. Wang, R. Ramesh, Nat. Mater. 7 (2008) 478.
[33] F. Gao, X.Y. Chen, K.B. Yin, S. Dong, Z.F. Ren, F. Yuan, T. Yu, Z.G. Zou, J.M. Liu, Adv. Mater. 19 (2007) 2889.
[34] S. Farhadi, M. Zaidi, J. Mol. Catal. A: Chem. 299 (2009) 18.
[35] H. Bader, V. Strurzenegger, J. Hoigne, Water Res. 22 (1988) 1109.
[36] X. Wang, S.H. Li, Y.S. Jiang, Inorg. Chem. 43 (2004) 6479.
[37] D. Banerjee, A.L. Markley, T. Yano, A. Ghosh, P.B. Berget, E.G. Minkley Jr., S.K. Khetan, T.J. Collins, Angew. Chem. Int. Ed. 45 (2006) 3974.
[38] A. Ghosh, D.A. Mitchell, A. Chanda, A.D. Ryabov, D.L. Popescu, E.C. Upham, G.J. Collins, T.J. Collins, J. Am. Chem. Soc. 130 (2008) 15116.
[39] W.P. Kwan, B.M. Voelker, Environ. Sci. Technol. 37 (2003) 1150.
[40] D.H. Bremner, R. Molina, F. Martinez, J.A. Melero, Y. Segura, Appl. Catal. B: Environ. 90 (2009) 380.